RENAL FAILURE
2022, VOL. 44, NO. 1, 1754–1768
https://doi.org/10.1080/0886022X.2022.2135446

Taylor & Francis
Taylor & Francis Group

LABORATORY STUDY

OPEN ACCESS Check for updates

Regulation of the autophagy plays an important role in acute kidney injury induced acute lung injury

Ruolin Wang[a]*, Siheng Shen[a]*, Luyong Jian[a], Shuhua Liu[b], Qi Yuan[a], Huahui Guo[a], Jiasheng Huang[a], Penghui Chen[a] and Renfa Huang[a]

[a]Nephropathy Department, Shenzhen Hospital (Futian) of Guangzhou University of Chinese Medicine, Shenzhen, China; [b]The Third Clinical Medical School, Guangzhou University of Chinese Medicine, Guangzhou, China

ABSTRACT

Aim: This study aimed to investigate the regulatory role of autophagy in acute kidney injury (AKI) induced acute lung injury (ALI).

Methods: The male Sprague–Dawley rats were divided into four groups: normal saline-treated sham rats (sham group), normal saline-treated ischemia-reperfusion injury rats (IRI group), 3-methyladenine-treated IRI rats (3-MA group), and rapamycin-treated IRI rats (RA group). The rats in the IRI rat model received the nephrectomy of the right kidney and was subjected to 60 mins of left renal pedicle occlusion, followed by 12, 24, 48, and 72 h of reperfusion. The levels of Scr, BUN, wet-to-dry ratio of lung, inflammatory cytokines, and oxidative stress were determined. The damage to tissues was detected by histological examinations. The western blot and immunohistochemistry methods were conducted to determine the expression of indicated proteins.

Results: Renal IRI could induce the pulmonary injury after AKI, which caused significant increases in the function index of pulmonary and renal, the levels of inflammatory cytokines, and biomarkers of oxidative stress. In comparison to the IRI group, the RA group showed significantly decreased P62 and Caspase-3 expression and increased LC-II/LC3-I, Beclin-1, Bcl-2, and unc-51-like autophagy activating kinase 1 expression. Meanwhile, by suppressing the inflammation and oxidative stress, as well as inhibiting the pathological lesions in kidney and lung tissues, the autophagy could effectively ameliorate IRI-induced AKI and ALI.

Conclusions: Autophagy plays an important role in AKI-induced ALI, which could be used as a new target for AKI therapy and reduce the mortality caused by the complication.

ARTICLE HISTORY
Received 31 May 2022
Revised 6 October 2022
Accepted 6 October 2022

KEYWORDS
Autophagy; apoptosis; ischemic reperfusion injury; acute kidney injury; acute lung injury

Introduction

Acute kidney injury (AKI) is one of the most common complications with various serious conditions [1], and a serious threat to human health due to the high cost and mortality [2]. The diagnosis of AKI is traditionally based on the serum creatinine (Scr) level and the estimated glomerular filtration rate. Additionally, blood urea nitrogen (BUN) levels, fractional sodium excretion, and proteinuria were also used for the diagnosis of AKI [3]. Renal ischemia-reperfusion injury (IRI) is most commonly involved in the pathophysiology of AKI, inducing the recruitment of inflammatory cells. With the release of numerous proinflammatory factors, the inflammatory cascade response initiates and participates in the occurrence and development of AKI [4]. Subsequently, these inflammatory factors enter the blood stream, bringing the damages to remote organs through the inflammatory response and oxidative stress. Acute lung injury (ALI) is considered as a major remote organ dysfunction caused by AKI due to the abundance of blood flow into the lung and the lung tissues are sensitivity to inflammatory damage, which is significantly connected to the prognosis of AKI [4]. ALI is a series of lung dysfunctions caused by a wide variety of lung injuries, thus having high morbidity and mortality [5]. Based on the accumulated publications, ALI is characterized by diffuse alveolar injury, lung edema formation, neutrophil-derived inflammation, and surfactant dysfunction [6]. The mortality of AKI-induced ALI is significantly high (more than 80%), thus leading to a worse prognosis than the simultaneous damage caused to any other remote organs [7]. Therefore, exploring new potential targets for the

CONTACT Renfa Huang huangrenfa1972@163.com Beihuan Avenue, Futian District, No. 6001, Shenzhen, China
*These authors have contributed equally to this work and share first authorship.

treatment and therapy of AKI-induced ALI is urgently needed.

Autophagy is a protective mechanism that is involved in the maintenance of cellular homeostasis and cell survival by keeping the function of the organs and degrading toxic waste products of cells. Autophagy-related proteins constitute the molecular machinery of the autophagy. The initiation of autophagy activation is mainly dependent on unc-51-like autophagy activating kinase 1 (ULK1). Combined with phosphatidylinositol 3-hydroxy kinase, Beclin-1 could significantly promote the initiation of autophagy. Furthermore, the activation of autophagy is positively correlated with the light chain (LC) 3 II/LC 3 I ratio and negatively associated with the expression of P62 [8]. Existed studies also indicted that autophagy is closely connected to the disease of kidney. Gur et al. found that the reduction of the autophagy is tightly associated with the worsens tubular injury and renal function [9]. The study by Bhatia et al. showed that through degrading damaged mitochondria, autophagy could significantly maintain the homeostasis of mitochondria, which is significantly involved in the survival of renal cells and the stabilization of kidney functions [10].

Whether autophagy plays a protective or damaging role in renal IRI is still controversial. At present, it is generally believed that autophagy could protect against renal IRI and renal IRI-caused AKI, but the exactly underlying mechanism has not completely clarified yet, and further studies are needed. Additionally, a complex association of the autophagy with the lung disease, like ALI, has been observed by several published studies [11]. The enhancement of the autophagy could effectively impair the inflammation and oxidative stress in the sepsis-induced ALI model and IRI lung tissues, suggesting the participation of autophagy in the process of ALI through anti-inflammation and anti-oxidation [12]. Zhan et al. proved that the autophagy might play a protective role in myocardial IRI-induced ALI by inhibiting inflammation [13]. However, the specific mechanisms underlying this association have not been determined. Although the above studies on autophagy have been thoroughly described, little is known about whether autophagy participates in the process of lung injury caused by AKI.

Based on these evidences, we hypothesized that autophagy plays a role in the development of lung injury after AKI through inflammation and oxidative stress. To confirm this hypothesis, we used a classic renal IRI model and investigated the levels of proteins related with the autophagy in the tissues of kidney and lung to identify the effect of autophagy on ALI after AKI.

Materials and methods

Experimental drug intervention

In this study, 3-methyladenine (3-MA) and rapamycin (RA) were used to inhibit and promote autophagy respectively. To determine the effect of autophagy on the functions of lung and kidney after IRI, we treated the IRI rats with 3-MA (15 mg/kg, 1 mL) [14] or RA (2 mg/kg,1 mL) [15] 12 h before the operation and 12 h after the reperfusion. The rats treated with saline were used as negative control. The vehicle for RA and 3-MA is saline.

Animals

A total of 48 healthy and clean eight-week-old male Sprague–Dawley rats weighed 200 ± 20 g were purchased from Guangdong Medical Experimental Animal Center with Animal License No.SCXK (Guangdong) 2018-0002. The rats were raised in the Animal Experiment Department of the laboratory of Guangzhou University of Chinese Medicine under the conditions of 25 ± 2 °C and 55 ± 5% humidity with 12/12 h light/dark cycles. All rats unrestricted access to standard diet and water. All the experimental procedures used for animal experiments in this study complied with the normative requirements of the animal ethics committee of the Guangzhou University of Chinese Medicine (approval No: 20201011002). The experimental animals were anesthetized before anatomical sampling and sacrificed after the end of the experiment.

Induction of renal IRI

The 48 Sprague–Dawley rats were randomly divided into four groups: normal saline (NS)-treated sham rats (sham group), NS-treated IRI rats (IRI group), 3-MA-treated IRI rats (3-MA group), and RA-treated IRI rats (RA group). Briefly, the rats were anesthetized using 2% pentobarbital sodium (0.3 mL/100 g), followed by bilateral abdominal incisions to excise and collect the right kidneys as the controls. After a stabilization period about 10 min, the left renal artery was separated and the left kidney was subjected to 60 min of ischemia using an atraumatic vascular clamp. The rats were placed in warming stations during the operation. Subsequently, the rats were treated with RA (2 mg/kg,1 mL) or 3-MA (15 mg/kg, 1 mL) or equal volume of saline 12 h before and after the surgery. The rats of the sham group were subjected to the same surgical procedure without clamping of the left renal vessels and

received equal volume of saline. At 12, 24, 48, and 72 h after IRI, the rats in each group ($n = 3$) were anesthetized again with 2% pentobarbital sodium (0.3 mL/100 g), followed by the collection of the abdominal aortic blood and bronchoalveolar lavage fluid (BALF). The serum and supernatant were separated and frozen at −80 °C after centrifugated. In addition, the tissue samples of lung and kidney were cryopreserved in liquid nitrogen for use in further experiments.

Detection of renal function

A biochemical autoanalyzer (Roche COBAS C501, Germany) was used to determine the levels of Scr and BUN in serum to evaluate the functions of kidney.

Evaluation of the wet-to-dry ratio of lung tissues

The lung water content was calculated as the ratio of wet weight to dry weight (W/D ratio): lung water content = ((wet weight − dry weight)/wet weight * 100%), representing the level of water content of the lung tissues. The right part of the lung was collected for the calculation of the W/D ratio.

The detection of serum and BALF

The concentrations of Interleukin-1β (IL-1β), tumor necrosis factor α (TNF-α), superoxide dismutase (SOD), malonaldehyde (MDA) and myeloperoxidase (MPO) were measured by enzyme-linked immunosorbent assay (ELISA) following the manufacturer's instructions (J&L Biomedical, Shanghai, China) at a wavelength of 450 nm.

Evaluation of renal damage and lung injury

In this study, we assessed the damage to tissues through histological examinations. Both samples of the kidney and lung were excised at specific time points as described above. Subsequently, a third of the samples was snap-frozen in liquid nitrogen and stored at −80 °C, another one third was fixed in 2% glutaraldehyde, and the remaining was fixed in 4% paraformaldehyde phosphate buffer solution overnight. After dehydrated by a graded series of ethanol, transverse kidney slices were embedded in the paraffin and cut into 5 μm-thick sections.

Kidney sections were stained with Periodic Acid-Schiff (PAS) for histopathological analysis. Ten fields (×400, 1 mm^2/field) per section were observed in the outer stripe of the outer medulla and examined by pathologists. Histopathological changes were scored based on the percentage of injured renal tubules. The semi-quantitative scores are as follows: 0, no injury; 1, less than 10%; 2, less than 25%; 3, less than 45%; 4, less than 75%; and 5, higher than 75%. The observed histological changes included the effacement and the loss of the proximal tubule brush border, the patchy loss of tubule cells, the focal areas of proximal tubular dilation, and the distal tubular casts, as well as the areas of cellular regeneration [16].

For the histopathological analysis of the lung tissues, hematoxylin and eosin (H&E) staining was performed. Three to five fields (×400, 1 mm^2/field) per section were observed by pathologists. Neutrophils have been found to be pivotal effectors of ALI and their depletion exerts a protective effect on AKI-induced ALI. Histopathological changes were scored based on the infiltration of neutrophil leukocyte and the change of the pulmonary architecture. The scores that ranged from 1 to 4 are as follows: grade 1 indicated normal histopathology; grade 2 indicated a low level of neutrophil leukocyte infiltration; grade 3 indicated moderate levels of neutrophil leukocyte infiltration, perivascular edema formation and partial destruction of the pulmonary architecture; while grade 4 indicated dense neutrophil leukocyte infiltration, abscess formation, and complete destruction of the pulmonary architecture [17]. The histology images were randomly selected, and the images of the following other methods were also randomly selected.

Transmission electron microscopy

For the analysis of the ultrastructure and observation of the autophagosomes, the samples were polymerized, cut and observed under a transmission electron microscopy (TEM) (TECNA-10, Philips, Netherlands).

Terminal 2-Deoxyuridine 5-Triphosphate Nick End-Labeling Assay (TUNEL)

An *in situ* apoptosis detection kit (ROCHE, Beijing, China) was employed to detect the apoptotic cells in renal and lung tissues. The apoptosis of the renal and lung tissues was defined as the ration of TUNEL-positive cells to the total number of cells in ten fields per section (original magnification ×200).

Immunohistochemistry and Western blot analyses

To evaluate the expression of Beclin-1, B-cell lymphoma-2 (Bcl-2), LC3-II/LC3-I, ULK1, P62, and cysteinyl

aspartate specific proteinase 3 (caspase-3), the immunohistochemistry (IHC) and western blot (WB) detections were applied.

The paraffin-embedded 5 μm-thick sections of the kidney or lung were deparaffinized and rehydrated. Antigen retrieval was performed by boiling the samples in a citric acid buffer (pH 6) for 1.5 min and then kept still for 3 min. The slides were rinsed using phosphate buffered saline and then treated with 10% hydrogen peroxidase in the distilled water to block the activity of the endogenous peroxidase. After cooled, anti-ULK1 (1:300, Boster, Wuhan, Hubei, China), anti-Beclin-1 (1:200, Boster, Wuhan, Hubei, China), anti-P62 (1:200, Boster, Wuhan, Hubei, China), anti-Bcl-2 (1:100, Boster, Wuhan, Hubei, China), anti-Caspase3 (1:100, Boster, Wuhan, Hubei, China), and anti-microtubule-associated proteins A/B (LC3A/B) (1:100, Boster, Wuhan, Hubei, China) antibodies were added and the sections were incubated in an incubator at 37 °C for 1 h. Subsequently, the sections were washed and incubated with a secondary biotinylated goat anti-rabbit antibody (1:5000; Proteintech) in an incubator at 37 °C for 25 min. Streptavidin-horse reddish peroxidase was added. The coloration was revealed using diaminobenzidine along with a substrate chromogen system (Dakocytomation), and the hematoxylin was used for nuclear counterstaining. As the final step, the nitrotyrosine intensity of the tissues of the kidney and lung were quantified using NIH ImageJ software.

For WB analysis, the protein samples were immediately placed in an ice-cold ristocetin-induced platelet aggregation buffer (150 mM NaCl, 50 mM Tris-HCl, 1 mM ethylenediaminetetraacetic acid, and 1% Triton X-100; pH 7.4) for 10 min after homogenized in a Dounce homogenizer, followed by the centrifugation for 10 min at 12,000 g/min, with the supernatant collected. The protein samples of the kidney and lung were respectively mixed in a Laemmli loading buffer and the mixture was boiled for 10 min and then subjected to sodium dodecyl sulfate polyacrylamide gel electrophoresis. Subsequently, the proteins were transferred onto a polyvinylidene fluoride membrane (ImmobilonP; Millipore, Bedford, MA) in a transfer buffer (25 mmol Tris, 0.2 mol glycine, and 20% methanol) using the wet transfer unit of the X cell SureLock system and blotted overnight against ULK1 (1:1,000), LC3-II/LC3-I (1:500), Beclin-1 (1:500), Bcl-2 (1:500), P62 (1:500), Caspase-3 (1:500), and glyceraldehyde-3-phosphate dehydrogenase (GAPDH) (1:10,000). Then, the membranes were washed using phosphate-buffered saline containing 0.05% TWEEN-20 and were incubated with a secondary antibody (1:1000 dilution) for 2 h. The protein bands were visualized using a chemiluminescence reaction. Densitometry analysis of the bands was performed using ImageJ software.

Statistical analysis

All the values in this study were expressed as mean ± SD and analyzed using SPSS 15.0 software. The paired *t*-test was used to determine intragroup mean values. One-way ANOVA was used for intergroup mean comparison. A value of p less than .05 was considered statistically significant.

Results

Autophagy in rats with AKI or AKI-induced ALI

According to previous studies, the autophagosome can be identified by the limiting membrane that is partially visible as two bilayers separated by a narrow electron-lucent cleft. The observations from TEM detection revealed that the autophagosomes are formed in the cells of the tissues of both renal and lung after IRI, accompanied by serious pathological changes in renal tissues. The nucleus was deformed and the epithelial cells had fallen off. However, the lipid droplets and vacuoles were occasionally observed in the cells. The pathological changes in the lung tissues were more serious, with the necrosis and deformation of the nucleus, large cell gaps, and lamellar body vacuoles. Furthermore, compared to that of rats from the IRI group, more autophagosomes were observed in the IRI rats treated with RA, while almost no autophagosomes were observed in the rats from the sham group. Additionally, compared to that of the rats from the IRI group, the rats of the 3-MA group showed significantly decreased amount of the autophagosomes, while tissue lesions were dramatically serious. The results showed the same trend at all time points (Figure 1).

IHC and WB analysis revealed that, compared to the rats of the sham group at any time points, the rats of the IRI group exhibited significantly increased the expression of ULK1, LC3-II/LC3-I, and Beclin-1. Moreover, in comparison to the rats of the IRI group, significantly high and low ULK1, LC3-II/LC3-I, and Beclin-1 expressions were observed in the rats of the RA group and the 3-MA group respectively. Meanwhile, opposite trend of P62 expression was also observed. Compared to the sham group, we observed significantly decreased P62 expression in the rats of the IRI group. Additionally, we also observed dramatically reduced and elevated P62 expression in the rats of the RA group and the 3-MA group, respectively, in

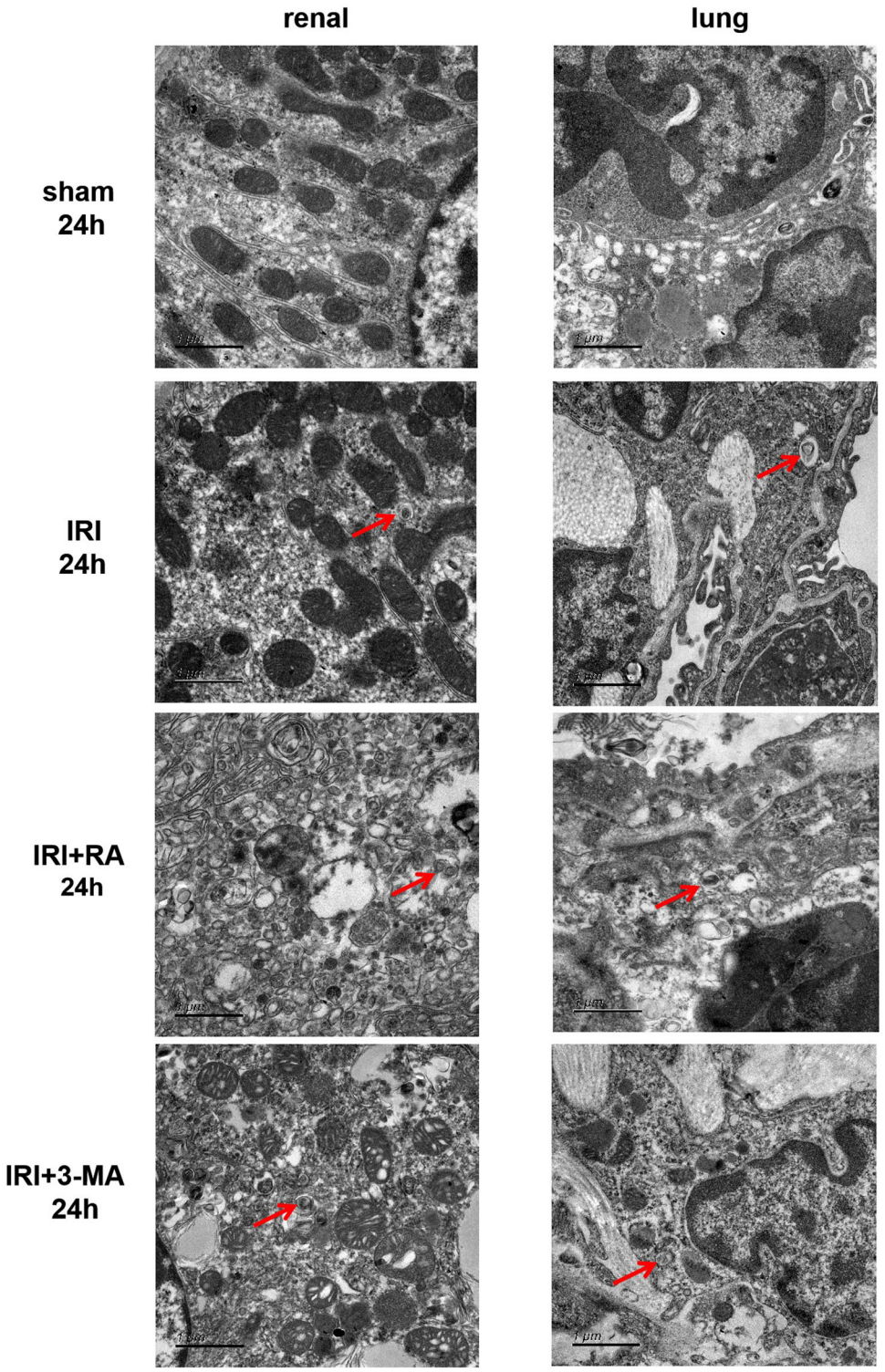

Figure 1. The result of transmission electron microscopy at 24 h after reperfusion. Red arrows point to the autophagosome.

comparison to the rats of the IRI group. The above-mentioned results were observed in the tissues of both the lung and kidney. These results clearly indicated that IRI can induce the autophagy, RA can activate the autophagy, and 3-MA could effectively inhibit the autophagy (Figures 2 and 3). Due to the peak of the kidney injury at 24 h after induction, the images of 24 h were selected to show.

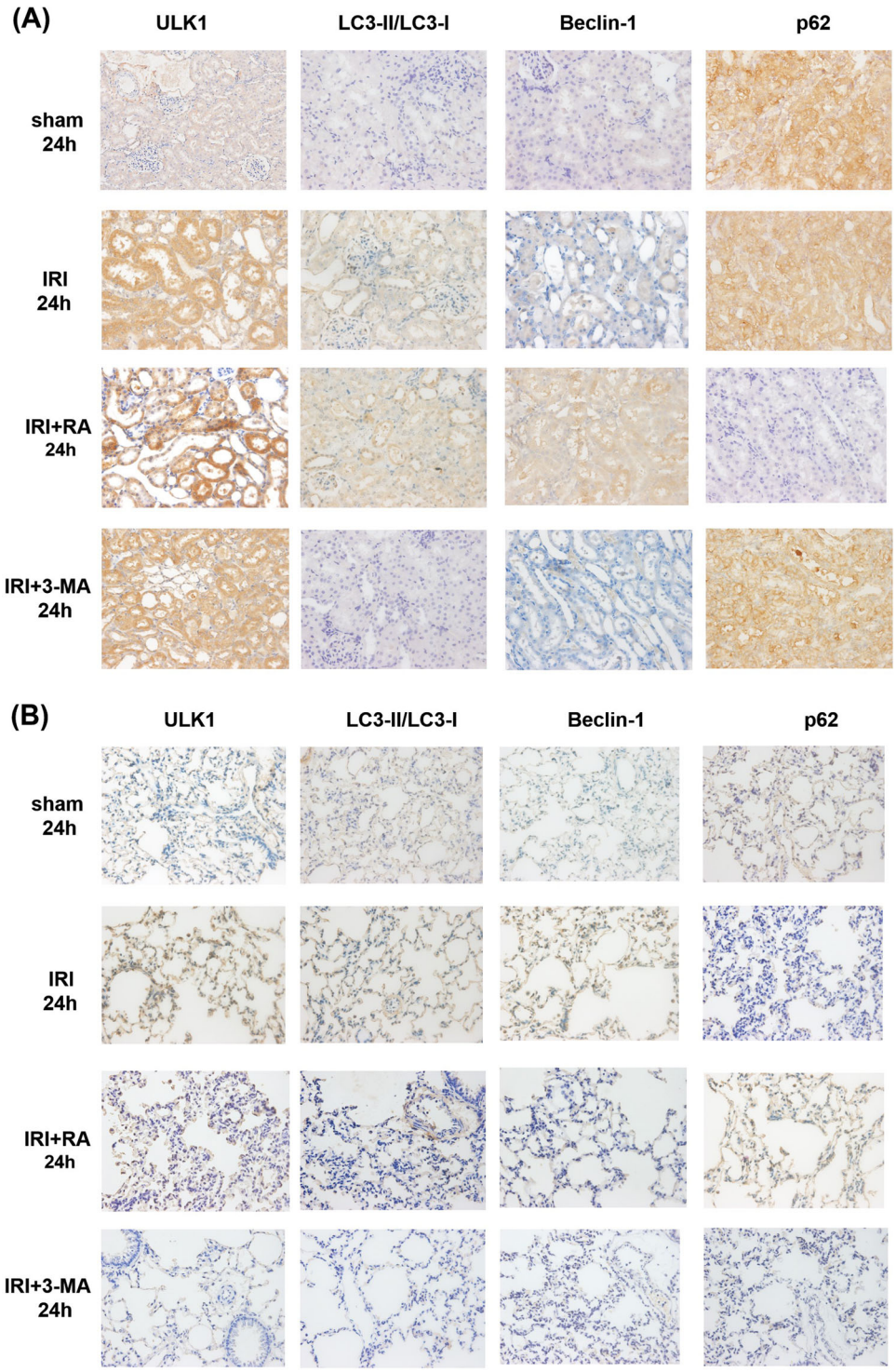

Figure 2. IHC results of autophagy-related proteins at 24 h after IRI. (A) Representative images showing the IHC results of kidney tissues. (B) Representative images showing the IHC results of lung tissues.

Autophagy protects rats against IRI-AKI

Compared to the sham group, the rats of the IRI group showed significantly high BUN and Scr production after reperfusion, and both peaking at 24 h. Additionally, in comparison to the rats of the IRI group, the rats of the 3-MA group and the RA group exhibited significantly high and low BUN and Scr production, respectively (Figure 4), suggesting the protective effect of autophagy promotion on IRI-caused renal dysfunctions.

In addition, the IRI-induced tubulointerstitial injury was also observed by the PAS staining, including in the focal areas of proximal tubular dilation and distal tubular casts, the effacement and loss of the proximal tubule brush

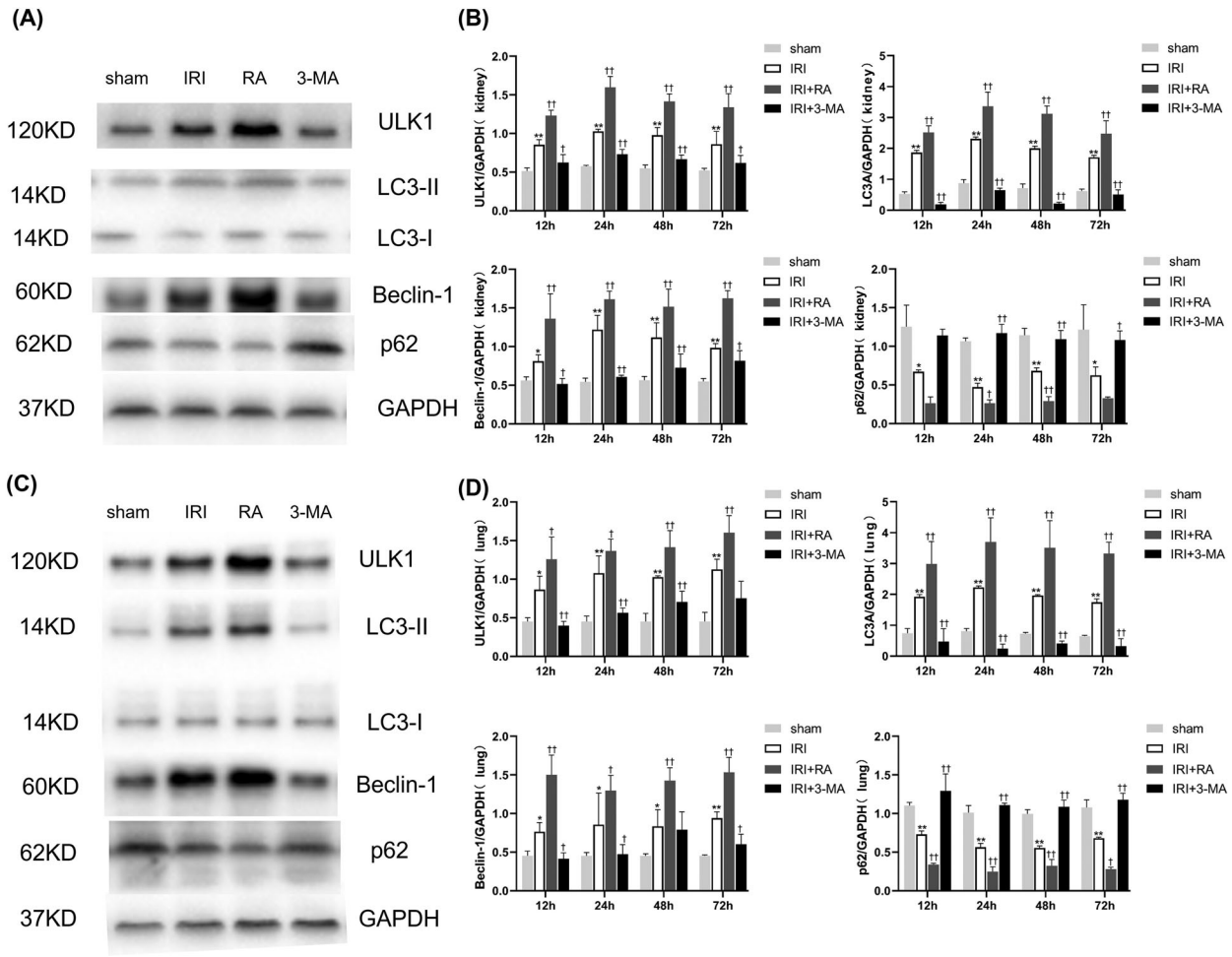

Figure 3. WB results of autophagy-related proteins. $^{*}p < .05$, it indicates that compared to the sham group. $^{**}p < .01$, it indicates that compared to the sham group. $^{\dagger}p < .05$, it indicates that compared to the IRI group. $^{\dagger\dagger}p < .01$, it indicates that compared to the IRI group. (A) WB images of ULK1, LC3-II/LC3-I, Beclin-1, and P62 in the kidney at 24 h after IRI. (B) Relative expression of ULK1, LC3-II/LC3-I, Beclin-1, and P62 in the kidney. (C) WB images of ULK1, LC3-II/LC3-I, Beclin-1, and P62 in the lung at 24 h after IRI. (D) Relative expression of ULK1, LC3-II/LC3-I, Beclin-1, and P62 in the lung.

border, and the infiltration of interstitial inflammatory cells. The degree of renal injury was scored using a range from 0 to 5, and the results showed that there was significantly higher damage in the 3-MA group compared to that in the IRI group. Meanwhile, it was also observed that renal histopathology produced the lower semi-quantitative scores along with less loss of brush borders, tubular dilation, and cast formation in the RA group than that in the IRI group (Figure 5). These results indicated that the suppression of autophagy could significantly enhance the IRI-induced tissue damage.

Autophagy mitigates AKI-induced ALI

As an important parameter of lung injury, the W/D ratio of lung was measured to determine the condition of pulmonary edema. Compared to the rats of the sham group, we observed a significantly high W/D ratio in the rats of the IRI group. Furthermore, compared to that of the rats from the IRI group, the rats from the RA group and the 3-MA group exhibited dramatically decreased and increased W/D ratio, indicating that the level of pulmonary edema in the RA group was the least serious (Figure 6).

Moreover, the results of the inflammatory cells infiltration and the damage of lung tissue structure showed that compared to the sham group, a small number of infiltrated inflammatory cells in the alveolar cavity and a slightly widened alveolar septum were discovered in the rats of the IRI group, but not significantly widened alveolar septum or disorganization of the alveolar structure in the IRI group. Additionally, compared to the rats of the IRI group, the rats of the RA group and 3-MA group showed dramatically reduced and increased inflammatory cells infiltration respectively. This result was also supported by the observation of the alveolar

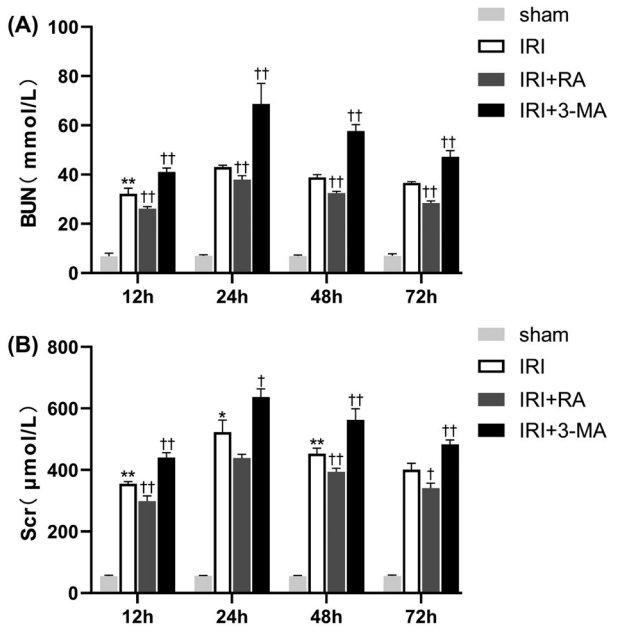

Figure 4. Renal function detection. $^{*}p < .05$, it indicates that compared to the sham group. $^{**}p < .01$, it indicates that compared to the sham group. $^{\dagger}p < .05$, it indicates that compared to the IRI group. $^{\dagger\dagger}p < .01$, it indicates that compared to the IRI group. (A) Blood urea nitrogen (BUN) content of rats in each group at each time point. (B) The serum creatinine (Scr) content of rats in each group at each time point.

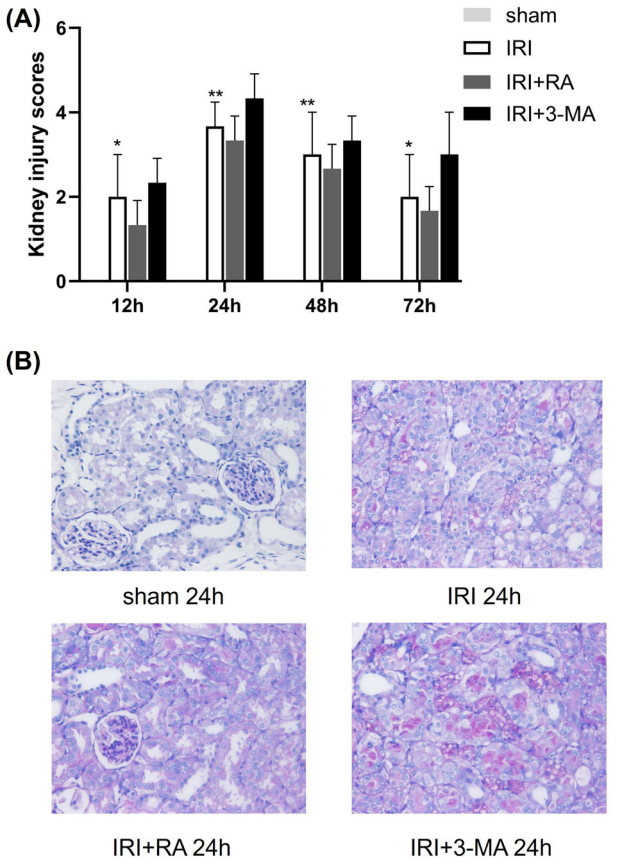

Figure 5. Histopathology of the kidney. $^{*}p < .05$, it indicates that compared to the sham group. $^{**}p < .01$, it indicates that compared to the sham group. (A) The results of semi-quantitative scores according to PAS staining of the kidney. (B) Representative images showing the results of PAS staining of the kidney tissues at 24 h.

structure damage severities (Figure 7). All the results mentioned above demonstrated that the activation of autophagy can protect rats against AKI-induced ALI.

Effect of autophagy on inflammation and oxidation

Due to the important roles of the inflammation and oxidation in the initiation and development of IRI-induced AKI and ALI, the productions of the inflammatory cytokines and oxidative stress markers were determined by ELISA assays.

Compared to the rats of the sham group, the rats of the IRI group exhibited significantly elevated pro-inflammatory cytokines production, such as IL-1β and TNF-α, in serum (Figure 8(A)) and BALF (Figure 8(B)). Furthermore, in comparison the rats of the IRI group, the rats of the RA group and 3-MA group showed dramatically decreased and increased secretion of pro-inflammatory cytokines in serum (Figure 8(A)) and BALF (Figure 8(B)). There was a significant difference between 12 and 24 h, while there was a more significant difference between 48 and 72 h (Figure 8(A,B)).

Next, we detected the level of MDA and MPO in the serum and BALF to evaluate the effect of autophagy on IRI-caused oxidative stress. A significantly increased level of MDA and MPO was observed in the serum (Figure 8(C)) and BALF (Figure 8(D)) of the IRI group compared to those of the sham group. Furthermore, compared to the IRI group, dramatically reduced and elevated productions of MDA and MPO in serum (Figure 8(C)) and BALF (Figure 8(D)) were also observed in the RA group and 3-MA group respectively. Meanwhile, we also observed a opposite trend of the level of SOD in the indicated groups (Figure 8(C,D)).

Effect of the autophagy on the apoptosis of renal and lung tissues

Our results showed that the ratio of TUNEL-positive cells in the renal and lung tissues in the IRI group increased significantly compared to the sham group, and reached to the peak at 24 h after the surgery. The percentage of apoptotic cells was higher in the 3-MA group than that in the IRI group, while the ratio of TUNEL-positive cells in the RA group significantly reduced (Figure 9(A,B)). The TUNEL-positive cells most

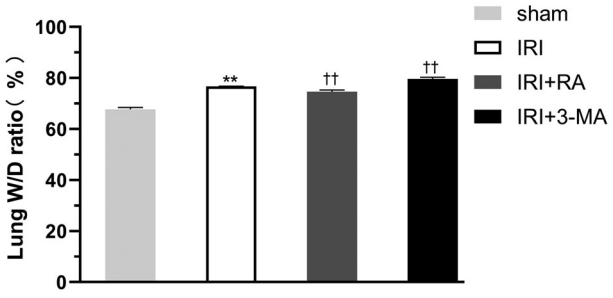

Figure 6. Lung water content of rats in each group (x ± SD, %). $^{**}p < .01$, it indicates that compared to the sham group. $^{††}p < .01$, it indicates that compared to the IRI group.

appeared in the renal cortex and all the part of the lung tissues (Figure 9(C,D)).

IHC and WB analysis revealed that compared to the IRI group at any time point, Bcl-2 expression in the RA group increased significantly, while the opposite result was observed for the expression of Caspase-3. On the contrary, compared to the IRI group, 3-MA significantly inhibited the degradation of Caspase-3, and suppressed the expression of Bcl-2 (Figure 10). These results demonstrated that when autophagy is promoted, apoptosis will be inhibited. In contrast, inhibiting autophagy will promote the occurrence of apoptosis.

Discussion

Previous studies have identified that the enhancement of autophagy can protect rats against AKI [18,19]. However, whether autophagy participates in AKI-induced ALI is not completely clarified. Our results revealed that autophagy can reduce the level of renal damage after IRI by reducing the inflammation and oxidative stress, manifested as a decreased production of inflammatory factors and mediators of oxidative damage. Meanwhile, the situation of apoptosis has been improved through the up-regulation of autophagy, and AKI-induced ALI was also ameliorated. As demonstrated by our findings, autophagy can protect rats from AKI-induced ALI by inhibiting inflammation, oxidative stress, and cell apoptosis.

AKI is a critical illness in clinic, in which the systemically released pro-inflammatory cytokines significantly increase, thus resulting in extensive cell injury, tissue damage [20], and subsequent injuries in distant organs [21]. ALI is the most critical remote organ dysfunction associated with AKI [22], and the mortality increases dramatically when both AKI and ALI occurred together [23]. In addition, the relationship between kidney injury and lung injury is bidirectional. AKI could negatively affect lung physiology by altering fluid balance, acid–base balance, and vascular tone [24]. Meanwhile, the

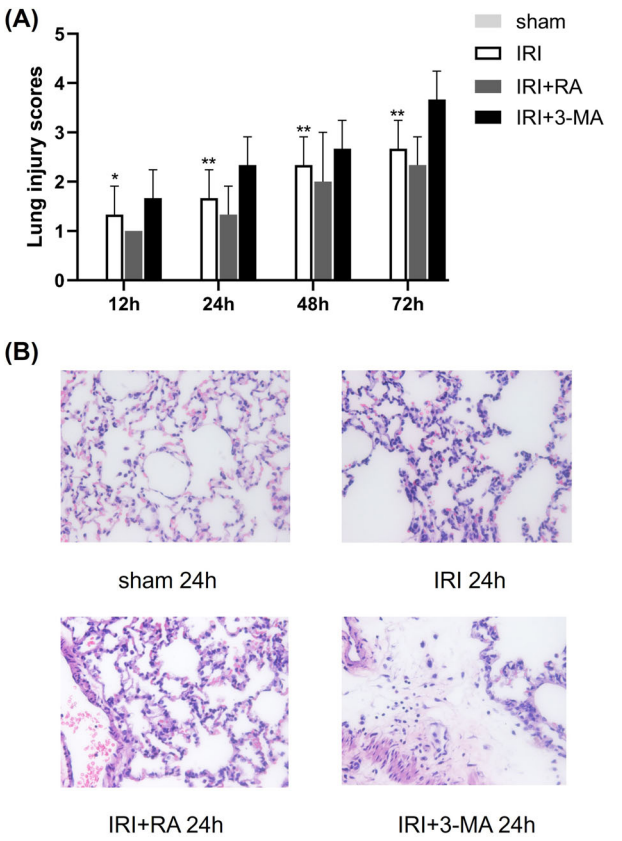

Figure 7. $^{*}p < .05$, it indicates that compared to the sham group. $^{**}p < .01$, it indicates that compared to the sham group. (A) The results of semi-quantitative scores according to H&E staining of the lung. (B) Representative images showing the H&E staining of lung tissues at 24 h.

kidney is highly sensitive to changes in partial oxygen pressure. The renin angiotensin aldosterone system is activated under hypoxic conditions, resulting in reduced renal blood flow and effective renal perfusion, leading to aggravated renal injury [25]. Our results showed that the kidney injury score reached to the peak at 24 h after surgery and then improved at 48 and 72 h, but the lung injury score got worse at each new time point. It showed that when inflammatory factors enter the bloodstream, the damage to the lung is irreparable and the lung injury will not stop even if kidney function is improved. Thus, discovering novel strategies to limit the development of AKI-induced ALI is urgently needed.

Autophagy serves as a dynamic recycling system that is associated with the pathologies of many human diseases, including AKI and ALI, and is an important mechanism underlying the maintaining of cellular homeostasis and survival under pathological stress conditions in the kidney [26]. The hallmark of the autophagy is the formation of autophagosomes and autolysosomes. Some studies have demonstrated that

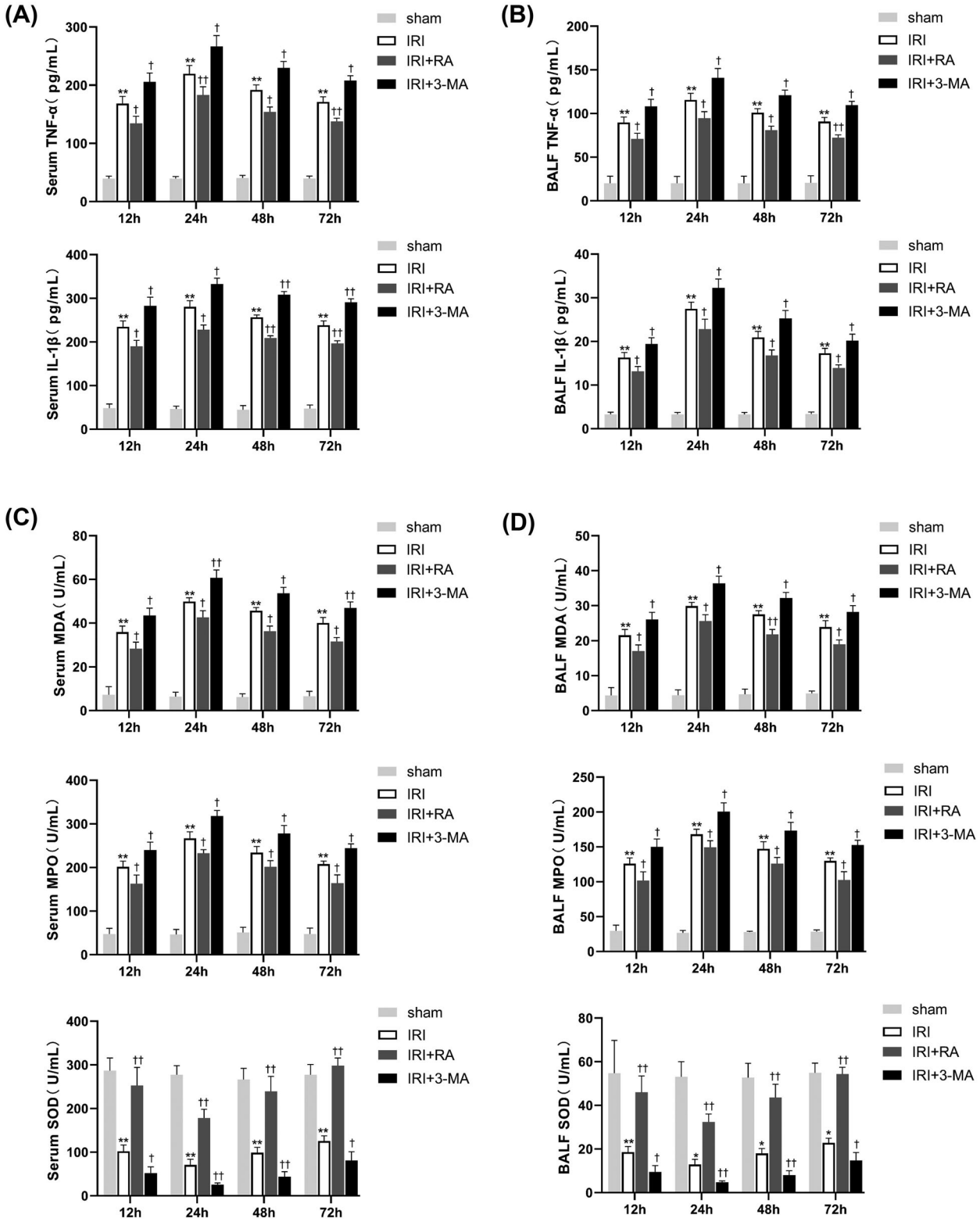

Figure 8. The levels of inflammatory factors and oxidative stress markers in serum and BALF. $^{*}p < .05$, it indicates that compared to the sham group. $^{**}p < .01$, it indicates that compared to the sham group. $^{\dagger}p < .05$, it indicates that compared to the IRI group. $^{\dagger\dagger}p < .01$, it indicates that compared to the IRI group. (A) Bar graphs showing the concentrations of indicated inflammatory factors in serum. (B) Bar graphs showing the concentrations of indicated inflammatory factors in BALF. (C) Bar graphs showing the levels of the oxidative stress-related markers in serum. (D) Bar graphs showing the levels of the oxidative stress-related markers in BALF.

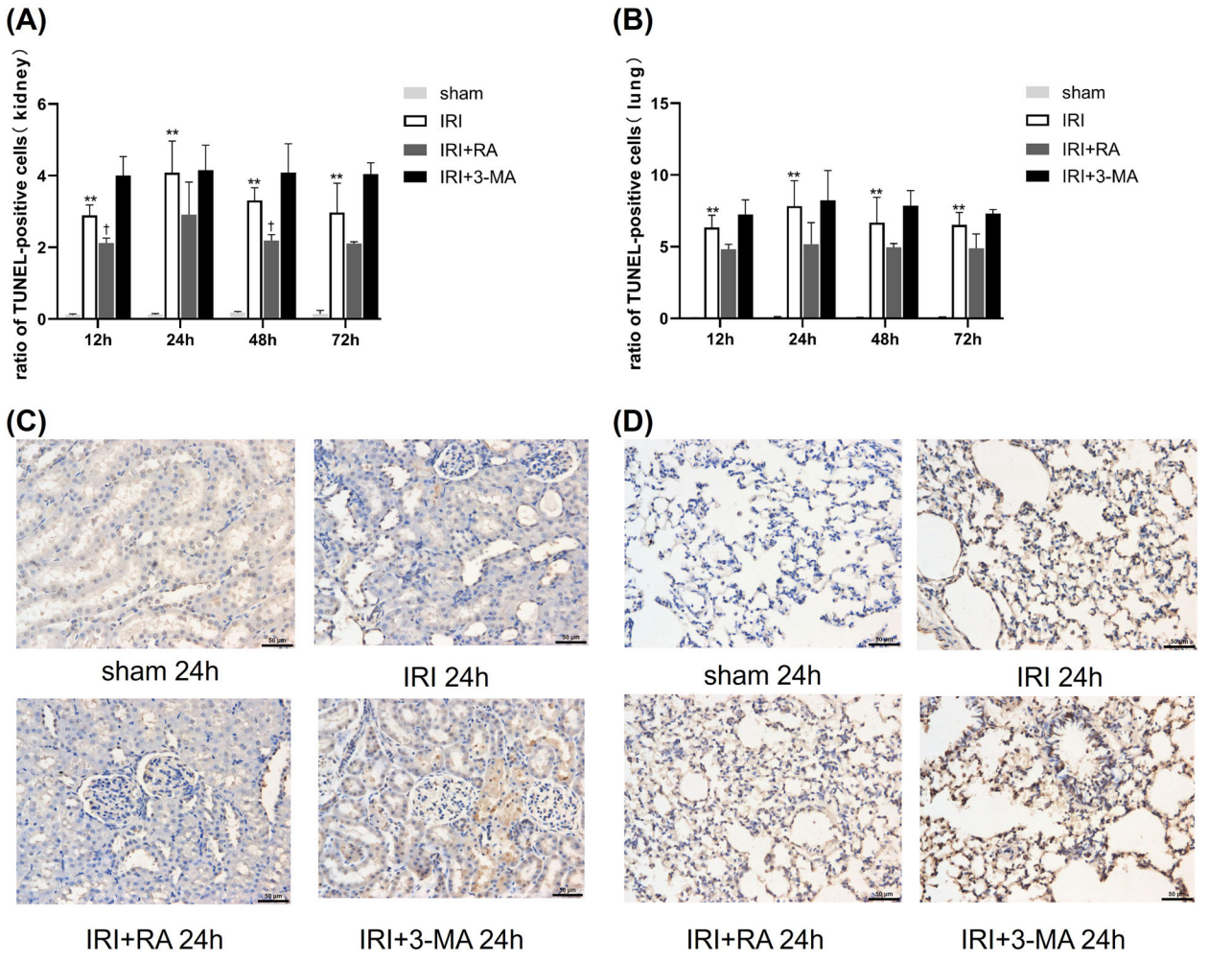

Figure 9. The ratio of TUNEL-positive cells (number of apoptotic cells/ (number of apoptotic cells + number of non-apoptotic cells) × 100%). $^{**}p < .01$, it indicates that compared to the sham group. $^{\dagger}p < .05$, it indicates that compared to the IRI group. (A) The ratio of TUNEL-positive cells in kidney tissues. (B) The ratio of TUNEL-positive cells in lung tissues. (C) Representative images showing the TUNEL-positive cells in the kidney tissues at 24 h. (D) Representative images showing the TUNEL-positive cells in the lung tissues at 24 h.

the formation of autophagosomes could be observed during the induction of autophagy under a TEM [27]. In addition, autophagy-related proteins are also important markers that can indicate the occurrence of autophagy. The initiation process of autophagy formation is mainly dependent on ULK1, which induces the induction of autophagy according to phosphorylation and ubiquitination [28].

Furthermore, many other autophagy-related proteins constitute the molecular machinery of autophagy, including Bcl-2/Beclin1 crosstalk and LC3-II/LC3-I turnover [29]. Mature LC3 is considered a marker of autophagy and is combined with phosphatidylethanolamine to form LC3-II, which then attaches to the autophagosome membrane, marking the formation of autophagosomes [30]. However, LC3-II is also degraded by lysosomes. This continuous turnover complicates the value of LC3-II as an indicator of autophagy and advocates the need for additional markers, such as the autophagy degradation substrate P62 [31]. P62 acts as a selective substrate and regulatory protein in mammals, binds directly to LC3-II, and is encapsulated by autophagosomes [32]. Therefore, an increase in autophagy is shown by an increased LC3-II/LC3-I ratio and a decreased P62 expression. Besides, Beclin-1 is also commonly used as an indicator for the detection of autophagy, which is combined with phosphatidylinositol 3-hydroxy kinase to promote autophagy under stress such as ischemia and hypoxia.

In our experiment, the expression of Beclin-1, ULK1, and LC3-II/LC3-I increased and the expression of p62 decreased in the RA group, and combined with the

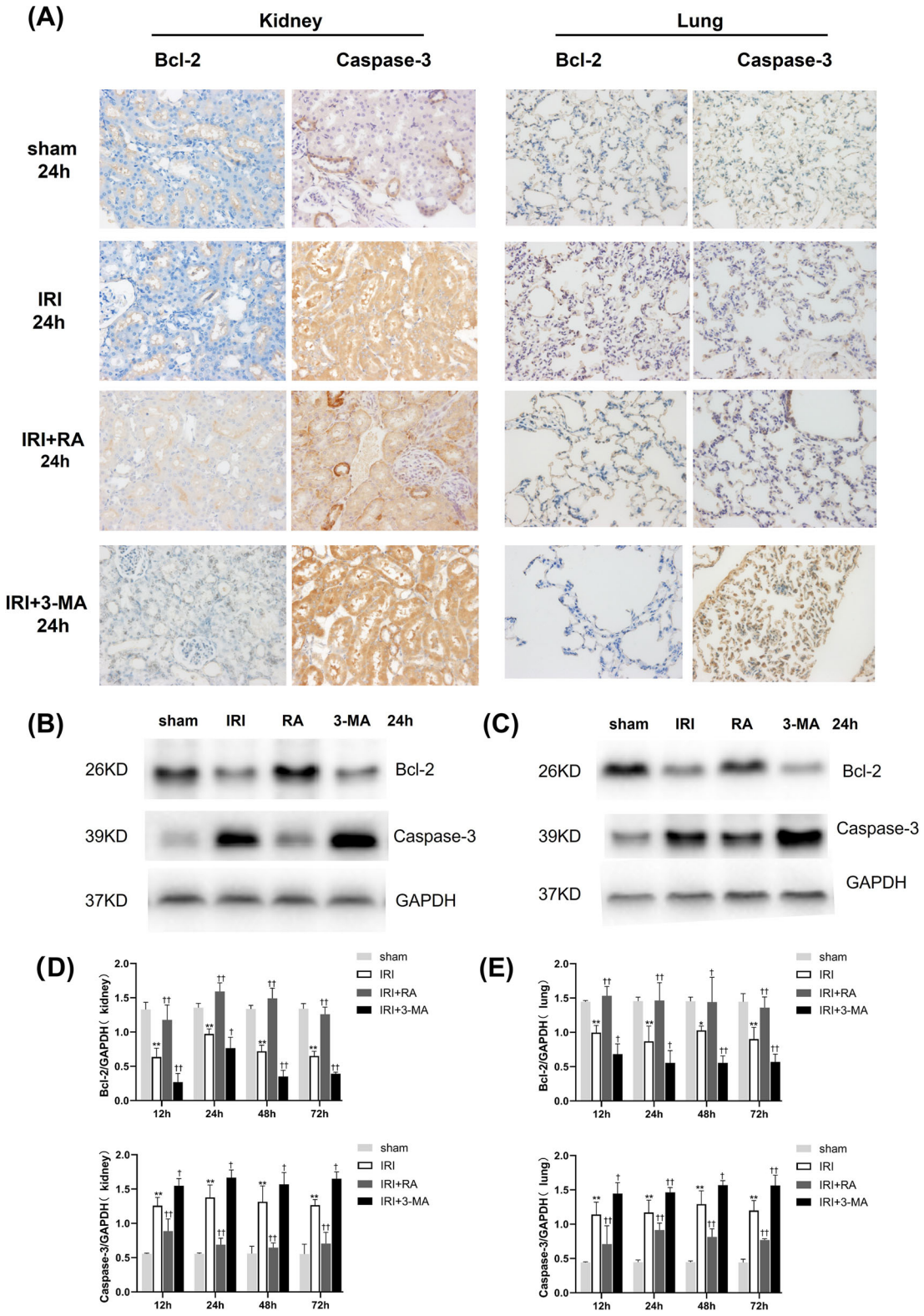

Figure 10. IHC and WB analysis of apoptosis proteins. $^{*}p < .05$, it indicates that compared to the sham group. $^{**}p < .01$, it indicates that compared to the sham group. $^{\dagger}p < .05$, it indicates that compared to the IRI group. $^{\dagger\dagger}p < .01$, it indicates that compared to the IRI group. (A) Representative images showing the expression of apoptosis-associated proteins in the kidney and lung tissues after IRI using IHC. (B) Representative blots showing the expression of Bcl-2 and Caspase-3 proteins in the kidney tissues after IRI. (C) Representative blots showing the expression of Bcl-2 and Caspase-3 proteins in the lung tissues after IRI. (D) Relative expression of Bcl-2 and Caspase-3 in the kidney tissues. (E) Relative expression of Bcl-2 and Caspase-3 in the lung tissues.

results of TEM, suggested that RA could promote autophagy and reduce lung and kidney injury caused by IRI. On the other hand, the expression of these proteins in the 3-MA group showed a opposite trend, suggested that promotive effect of autophagy inhibition on the lung and kidney injury. Meanwhile, the BUN, Scr, lung W/D ratio, and pathology of both kidney and lung tissues in the RA group all moved toward better, while these indicators in the 3-MA group all moved toward worse. All the above results demonstrated that autophagy is significantly involved in lung-kidney crosstalk and plays a positive role in AKI-induced ALI.

Research has shown that inflammation and oxidative stress are the main causes of AKI-induced organ damage. Following renal IRI, a large number of reactive oxygen species are produced and the expression of MDA is also increased. Once it exceeds the scavenging capacity of antioxidant enzymes, such as SOD, the apoptosis of renal tubular epithelial cells and pulmonary endothelial cells will be caused [33,34]. Therefore, the increase of MDA and the decrease of SOD indicate an increased oxidative stress and cell apoptosis. At the same time, a large number of studies have shown that renal IRI can induce the secretion of TNF-α, which could increase the production of inflammatory factors, such as IL-6, IL-8, and monocyte chemotactic protein-1, and activate cascade reactions involved in inflammation [35,36].

Neutrophil elastase (NE) is the ultimate effector of the inflammatory cascade in ALI. A positive correlation is observed between NE and IL-1β [37]. Additionally, TNF-α is also related to NE [38]. To sum up, autophagy could effectively improve AKI or AKI-induced ALI by reducing the inflammatory response. Therefore, we observed a significant decrease in the expression of IL-1β and TNF-α, as well as markers of oxidative stress, such as MDA and MPO, while the expression of SOD showed a significant increase in the lung and kidney tissues of rats in the RA group. It can be inferred that the promotion of autophagy reduces the level of oxidative damage and inflammatory response in the lung and kidney after IRI and exerts a protective role in lung and kidney injury.

Autophagy and apoptosis are two important cellular processes. In many other cases, autophagy and apoptosis develop exclusively. However, autophagy and apoptosis may be triggered by common upstream signals, and sometimes these results in combined autophagy and apoptosis. Apoptosis is a programmed cell death, and its initiation is dependent on the activation of a series of cysteine-aspartic proteases known as Caspases. There are two categories of Caspases, including initiator Caspase and effector Caspase. Caspase-3 is an effector Caspase. Active caspase-3 is responsible for the final execution of proteolytic degradation of a variety of intracellular proteins [39]. Members of the Bcl-2 protein family are responsible for the regulation of apoptosis and are critical to the regulation of both intrinsic and extrinsic apoptotic pathways [40]. As mentioned above, Bcl-2 can combine with Beclin-1 to participate in the process of apoptosis. When autophagy is promoted, the degree of apoptosis will be reduced accordingly. Our results showed that decreased Caspase-3, increased Bcl-2 and Beclin-1, represent the decreased apoptosis in lung and kidney tissues when autophagy was promoted. According to our results, we can speculate that autophagy not only plays a role in the lung-kidney crosstalk through anti-inflammatory and antioxidation, but also plays a protective role in the inhibition of apoptosis.

Conclusions

According to previous work, we generally believed that autophagy plays a protective role in renal IRI, but the mechanism is very complex. Inflammation and oxidative stress are the most critical pathophysiological processes involved in renal IRI-induced ALI, and both of these processes can induce autophagy. At the same time, autophagy and apoptosis also have an inseparable relationship. Our results indicated that autophagy exerts a protective role in ALI following AKI by antagonizing inflammation, oxidative stress, and apoptosis. Therefore, autophagy may be a novel and promising approach that can be used to limit kidney damage and subsequent AKI-induced ALI.

The strengths and limitations

Our study revealed that autophagy is activated in AKI-induced ALI and acts as a crucial positive regulator. At present, there is little research in this area. Therefore, this study may lead to new early prevention and diagnosis in AKI and AKI-induced ALI. However, there is still something that needs to be improved. First, our study was short of research about autophagy-related signaling pathway, and we plan to carry out subsequent experiments to investigate it. In addition, we plan to conduct further gene-related experiments and conduct more in-depth research in this area.

Author contributions

R-LW designed the experimental scheme, conceived and wrote the manuscript. S-HS collected materials and

participated in the experimental process. QY took part in the experimental process. L-YJ made the first revision of the manuscript. S-HL contributed to manuscript drafting. H-HG submitted the final manuscript. J-SH and P-HC participated in the experimental process. R-FH put forward theoretical ideas and modified the final manuscript. All authors participated in this article and finally approved the submitted and published version.

Disclosure statement

The authors have no conflicts of interest to declare.

Funding

This work was supported by the grants from the National Natural Science Foundation of China [No. 81460682, 81760805], the Natural Science Foundation of Guangdong Province [No. 2020A151501572], and the Shenzhen foundation of science and technology research and development [No. JCYJ20190809102413156].

ORCID

Ruolin Wang http://orcid.org/0000-0002-0348-5256
Siheng Shen http://orcid.org/0000-0002-3505-6683
Luyong Jian http://orcid.org/0000-0001-9233-4961
Shuhua Liu http://orcid.org/0000-0002-8633-5826
Qi Yuan http://orcid.org/0000-0002-7040-4612
Huahui Guo http://orcid.org/0000-0003-1106-5312
Penghui Chen http://orcid.org/0000-0001-8252-936X
Renfa Huang http://orcid.org/0000-0003-3096-4129

Data availability statement

All data included in this study are available upon request by contact with the corresponding author.

References

[1] Rossaint J, Zarbock A. Acute kidney injury: definition, diagnosis and epidemiology. Minerva Urol Nefrol. 2016;68(1):49–57.
[2] Zuk A, Bonventre JV. Acute kidney injury. Annu Rev Med. 2016;67:293–307.
[3] Ricci Z, Romagnoli S. Acute kidney injury: diagnosis and classification in adults and children. Contrib Nephrol. 2018;193:1–12.
[4] Haschler TN, Horsley H, Balys M, et al. Sirtuin 5 depletion impairs mitochondrial function in human proximal tubular epithelial cells. Sci Rep. 2021;11(1):15510.
[5] Mokrá D. Acute lung injury - from pathophysiology to treatment. Physiol Res. 2021;69(Suppl 3):S353–S366.
[6] Hughes KT, Beasley MB. Pulmonary manifestations of acute lung injury: more than just diffuse alveolar damage. Arch Pathol Lab Med. 2017;141(7):916–922.
[7] Faubel S, Edelstein CL. Mechanisms and mediators of lung injury after acute kidney injury. Nat Rev Nephrol. 2016;12(1):48–60.
[8] Cao W, Li J, Yang K, et al. An overview of autophagy: mechanism, regulation and research progress. Bull Cancer. 2021;108(3):304–322.
[9] Kaushal GP, Shah SV. Autophagy in acute kidney injury. Kidney Int. 2016;89(4):779–791.
[10] Bhatia D, Chung K-P, Nakahira K, et al. Mitophagy-dependent macrophage reprogramming protects against kidney fibrosis. JCI Insight. 2019;4(23):e132826.
[11] Qu L, Chen C, Chen Y, et al. High-mobility group box 1 (HMGB1) and autophagy in acute lung injury (ALI): a review. Med Sci Monit. 2019;25:1828–1837.
[12] Meng L, Zhao X, Zhang H. HIPK1 interference attenuates inflammation and oxidative stress of acute lung injury via autophagy. Med Sci Monit. 2019;25:827–835.
[13] Zhan L, Zhang Y, Su W, et al. The roles of autophagy in acute lung injury induced by myocardial ischemia reperfusion in diabetic rats. J Diabetes Res. 2018;2018:5047526.
[14] Liu H, Lei H, Shi Y, et al. Autophagy inhibitor 3-methyladenine alleviates overload-exercise-induced cardiac injury in rats. Acta Pharmacol Sin. 2017;38(7):990–997.
[15] Zhao J, Wang H, Yang H, et al. Autophagy induction by rapamycin ameliorates experimental colitis and improves intestinal epithelial barrier function in IL-10 knockout mice. Int Immunopharmacol. 2020;81:105977.
[16] Devarajan P. Update on mechanisms of ischemic acute kidney injury. J Am Soc Nephrol. 2006;17(6):1503–1520.
[17] Ozdulger A, et al. The protective effect of N-acetylcysteine on apoptotic lung injury in cecal ligation and puncture-induced sepsis model. Shock. 2003;19(4):366–372.
[18] Ji J, Zhou X, Xu P, et al. Deficiency of apoptosis-stimulating protein two of p53 ameliorates acute kidney injury induced by ischemia reperfusion in mice through upregulation of autophagy. J Cell Mol Med. 2019;23(4):2457–2467.
[19] Gong L, Pan Q, Yang N. Autophagy and inflammation regulation in acute kidney injury. Front Physiol. 2020;11:576463.
[20] Sato Y, Yanagita M. Immune cells and inflammation in AKI to CKD progression. Am J Physiol Renal Physiol. 2018;315(6):F1501–f1512.
[21] Kher A, Kher V. Prevention and therapy of AKI in asia: a big challenge. Semin Nephrol. 2020;40(5):477–488.
[22] Singbartl K. Renal-pulmonary crosstalk. Contrib Nephrol. 2011;174:65–70.
[23] Teixeira JP, Ambruso S, Griffin BR, et al. Pulmonary consequences of acute kidney injury. Semin Nephrol. 2019;39(1):3–16.
[24] Rossi M, Delbauve S, Roumeguère T, et al. HO-1 mitigates acute kidney injury and subsequent kidney-lung cross-talk. Free Radic Res. 2019;53(9-10):1035–1043.
[25] Basu RK, Wheeler DS. Kidney-lung cross-talk and acute kidney injury. Pediatr Nephrol. 2013;28(12):2239–2248.
[26] Kaushal GP, Chandrashekar K, Juncos LA, et al. Autophagy function and regulation in kidney disease. Biomolecules. 2020;10(1):100.

[27] Jiang M, Liu K, Luo J, et al. Autophagy is a renoprotective mechanism during in vitro hypoxia and in vivo ischemia-reperfusion injury. Am J Pathol. 2010;176(3): 1181–1192.
[28] Booth LA, Tavallai S, Hamed HA, et al. The role of cell signalling in the crosstalk between autophagy and apoptosis. Cell Signal. 2014;26(3):549–555.
[29] Decuypere J-P, Ceulemans LJ, Agostinis P, et al. Autophagy and the kidney: implications for ischemia-reperfusion injury and therapy. Am J Kidney Dis. 2015; 66(4):699–709.
[30] Glick D, Barth S, Macleod KF. Autophagy: cellular and molecular mechanisms. J Pathol. 2010;221(1):3–12.
[31] Liu L, Feng D, Chen G, et al. Mitochondrial outer-membrane protein FUNDC1 mediates hypoxia-induced mitophagy in mammalian cells. Nat Cell Biol. 2012; 14(2):177–185.
[32] Sánchez-Martín P, Saito T, Komatsu M. p62/SQSTM1: 'jack of all trades' in health and cancer. Febs J. 2019; 286(1):8–23.
[33] Aboutaleb N, Jamali H, Abolhasani M, et al. Lavender oil (lavandula angustifolia) attenuates renal ischemia/reperfusion injury in rats through suppression of inflammation, oxidative stress and apoptosis. Biomed Pharmacother. 2019;110:9–19.
[34] Hadj Abdallah N, Baulies A, Bouhlel A, et al. Zinc mitigates renal ischemia-reperfusion injury in rats by modulating oxidative stress, endoplasmic reticulum stress, and autophagy. J Cell Physiol. 2018;233(11): 8677–8690.
[35] Ramesh G, Reeves WB. Inflammatory cytokines in acute renal failure. Kidney Int Suppl. 2004;66(91): S56–S61.
[36] Kielar ML, John R, Bennett M, et al. Maladaptive role of IL-6 in ischemic acute renal failure. J Am Soc Nephrol. 2005;16(11):3315–3325.
[37] Alfaidi M, Wilson H, Daigneault M, et al. Neutrophil elastase promotes interleukin-1β secretion from human coronary endothelium. J Biol Chem. 2015; 290(40):24067–24078.
[38] Lee JM, Yeo CD, Lee HY, et al. Inhibition of neutrophil elastase contributes to attenuation of lipopolysaccharide-induced acute lung injury during neutropenia recovery in mice. J Anesth. 2017;31(3):397–404.
[39] Xu X, Lai Y, Hua ZC. Apoptosis and apoptotic body: disease message and therapeutic target potentials. Biosci Rep. 2019;39(1):BSR20180992.
[40] Cory S, Adams JM. The Bcl2 family: regulators of the cellular life-or-death switch. Nat Rev Cancer. 2002;2(9): 647–656.